Supporting Information

Direct visualization and functional characterization of *Gar2* ^{Nucleolin} -G-quadruplex interactions

Ajay Kumar[1], and Nasim Sabouri[1,2 #]

[1]Department of Medical Biochemistry and Biophysics, Umeå University, SE-901 87 Umeå, Sweden

[2]Science for Life Laboratory, Umeå University, Umeå, Sweden

[#] Corresponding author: nasim.sabouri@umu.se

Phone: +46 786 50 00

Material and Methods

Bacterial strains, culture and plasmids

All strains of *E. coli* were grown in LB media at 37 °C and appropriate antibiotics (50 µg/ml Kanamycin, 30 µg/ml Chloramphenicol) were added when required. All plasmids were maintained in *E. coli* DH-5α strain. All recombinant proteins were expressed in Rosetta (DE3) strain. *E. coli* strains and plasmids used in this study are included in Supporting Table S1and S2.

Yeast strains and culture

Wild type and genetically modified strains of *S. pombe* were grown in YES media at 30 °C and appropriate antibiotic G418 was added when required during strain construction. *S. pombe* strains used in this study are listed in Supporting Table S1.

Preparation of recombinant BG4 antibody

Recombinant BG4 antibody was prepared from the pSANG10-3F-BG4 plasmid[1]. The BG4 antibody was expressed and purified at the Protein Expertise Platform at Umeå University following a previously described protocol[2].

C-terminal tagging of gar2 gene in *S. pombe*

C-terminal 3xHA epitope (YPYDVPDYA) tagging of gar2 at its endogenous locus was performed using a modified PCR-based homologous recombination (HR) method[3]. To enhance homologous recombination efficiency, homology arms of up to 250 bp were used. Briefly, a linear PCR amplified cassette was generated by overlap extension PCR, in which 250 bp sequences upstream (UPS) and downstream (DNS) of the gar2 stop codon were fused to a 3xHA epitope tag and KanMX6 selectable marker (amplified from the pFA6a

plasmid). The resulting PCR product (UPS::3xHA-kanMX6::DNS) was purified and transformed into *S. pombe* cells using the lithium acetate method, and transformants were selected on YES agar containing 100 µg/ml G418[4]. Successful integration was verified by PCR using a gene-specific forward primer and a KanMX6 reverse primer, and the PCR product was further confirmed by Sanger sequencing. Expression of Gar2-3xHA was validated by Western blot analysis using anti-HA antibodies.

Cloning of Gar2 and its various mutants

The full-length gar2 gene (1500 bp encoding 500 amino acids) was amplified from *S. pombe* genomic DNA using Phusion DNA polymerase and cloned into NcoI and XhoI sites of pET24d expression vector. For deletion mutants of gar2, two constructs were generated : 1) the R1R2RGG variant (784-1500 bp encoding 263-500 amino acids) spanning RRM1, RRM2 and RGG motifs, 2) the R1R2 variant (784-1329 bp encoding 263-443 amino acids) spanning RRM1 and RRM2 motifs. Both fragments were amplified from genomic DNA and cloned into NcoI and XhoI sites of pET24d vector. Alanine substitutions in the RGG motif were introduced using site-directed mutagenesis to generate two variants: 1) the first variant named R>A generated by replacing five arginine residues by alanine as R450A/R453A/R459A/R465A/R476A. 2) the second variant named F>A generated by substituting phenylalanine residues with alanine as F456A/F462A/F468A. All constructs were verified by Sanger sequencing and transformed into Rosetta (DE3) cells for expression.

Protein expression and purification

Full-length Gar2 protein and its variants (R1R2RGG, R1R2, F>A, R>A) were expressed separately in *E. coli* Rosetta (DE3) strain. Briefly, Rosetta cells harbouring respective plasmid constructs were grown at 37 °C in LB media containing 50 µg/ml Kanamycin to

OD_{600} 0.4. The expression of recombinant proteins was induced by adding 0.2 mM IPTG at 22 °C for five hours. Cells were harvested and subjected to freeze-thaw cycles and lysed with a buffer containing 50 mM Hepes (pH 7.6), 500 mM NaCl, 10% glycerol, 0.02% Igepal detergent, 10 mM imidazole, 2 mM beta-mercaptoethanol (β-ME), 5 mM $MgCl_2$, 5 mM $CaCl_2$, 7.5 µg/ml DNaseI, 0.1 mg/ml lysozyme, protease inhibitor (Roche). Lysates were centrifuged at 15,000 RPM at 4 °C for 35 minutes (rotor: JA-25.50). The supernatant was incubated with Ni-NTA agarose (Qiagen) beads for an hour at 4 °C. The proteins captured on the beads were extensively washed with wash buffer (50 mM Hepes pH 7.6, 1 M NaCl, 10% glycerol, 30 mM imidazole, 2 mM β-ME). The bound proteins were eluted with buffer containing 50 mM Hepes pH 7.6, 500 mM NaCl, 10 % glycerol, 250 mM imidazole, 2 mM β-ME. The eluted protein was subjected to desalting with PD10 column (Cytiva). For full length Gar2 and all variants except R1R2, a second column purification with heparin beads was performed. The proteins from heparin column were eluted with NaCl gradient. The chromatograms of heparin purification are shown in Fig. S9A-D. R1R2 was purified solely via Ni-NTA as it did not bind to heparin column. Finally, proteins were buffer exchanged into 50 mM Hepes pH 7.6, 500 mM NaCl (required for solubility), 10 % glycerol, 2 mM β-ME and flash frozen. The purified proteins were subjected to SDS-PAGE and Coomassie staining to analyse their purity (Fig. S8E).

Immunoflourescence microscopy

Colocalization studies were performed using immunofluorescence microscopy as previously described with modifications. Briefly, exponentially growing *S. pombe* cells were fixed with 4% formaldehyde for one hour at 30 °C. Excess formaldehyde was removed by washing with PEM buffer (100 mM PIPES, 1 mM EGTA, 1 mM $MgSO_4$, pH 6.9). Cell wall was digested by resuspending the cells in PEMS (PEM + 1.2 M Sorbitol) containing 2.5 mg/ml Zymolyase 20T, 2.5 mg/ml lyticase and 5 mM β-ME at a final concentration of 2.5×10^7

cells/ml. The cells were incubated at 37 °C for 90 minutes to enable efficient cell wall digestion. Following digestion, the cells were permeabilized by treatment with 1% triton in PEMS for 20 minutes.

Unreacted aldehyde groups were quenched with 5 mg sodium borohydride in 15 ml PEM for five minutes followed by three PEM washes. Next, the cells were resuspended in PEMBAL buffer (1% BSA, 100 mM Lysine HCl, 0.1 % NaN_3) for 30 minutes at RT to block nonspecific binding. 1/5 of the cell suspension were transferred to the fresh Eppendorf tube, pelleted, and resuspended in PEMBAL containing BG4 antibodies (1:200 dilution) at 4 °C overnight. In experiments, where colocalization of G4 was performed with Gar2, cells were co-incubated with anti-HA (mouse) antibodies (1:500 dilution) and BG4 at this step. Unbound antibodies were removed by washing the cells with PEMBAL. The cells were resuspended in PEMBAL containing anti-FLAG (Rabbit) antibodies for two hours at RT. The unbound anti-FLAG antibodies were removed by washing with PEMBAL. Cells were incubated with Alexa Fluor 594 conjugated anti-Rabbit IgG (1:500 dilution) for two hours at RT. For the colocalization experiments, Alexa fluor 488 conjugated anti-mouse IgG (1:500 dilution) was also used and co-incubated with the anti-rabbit IgG to allow dual labeling. After antibody incubation, cells were stained with 1 µg/ml DAPI prepared in 1xPBS for five minutes at RT and washed twice with 1xPBS to visualize nuclei. Following DAPI staining, cells were adhered to poly-D-Lysine coated coverslips for ten minutes, air dried and mounted on glass slides using mounting media. Imaging was conducted using a Leica DMi8 wide field microscope equipped with a 100x/1.4 (NA) with oil immersion objective, an LED light source, and a CCD camera. Images were acquired with LAS X software using fixed exposure settings.

Immunoelectron microscopy

The procedure followed was adopted from previously published method with slight modifications[5]. Briefly, cells in log phase were pelleted down and fixed by chemical fixation (2% paraformaldehyde + 0.2 % glutraldehyde in 0.1 M PHEM buffer) for two minutes in a microwave (PELCO BioWave Pro+). Fixed cells were washed with 1% glycine in PBS, resuspended in gelatin and incubated at 37 °C for 30 minutes. The gelatin embeded pellet was sectioned into small pieces and infiltrated with 0.4 M sucrose at 4 °C overnight. The blocks were snap frozen in liquid nitrogen, and ulttrathin sections of 70 nm were cut at -120 °C using a Leica EM UC7 cryo-ultramicrotome equipped with a diamond knife (DiATOME). Sections were picked up using a mixture of 2% methyl cellulose and 2.3 M sucrose and transferred to formavar-coated hexagonal copper EM grids (TAAB Laboratories Equipment Ltd). Gelatin and metal cellulose were removed by incubating the grids in PBS at 37 °C for 30 minutes followed by washing in PBS and quenching with glycine. After an additional PBS wash, grids were blocked with 1% fish skin gelatin (Sigma G7041) and 1% acetylated BSA (Sigma B2618)] in PBS. Grids were incubated with appropriate primary (either BG4 or anti-HA or both) and secondary (anti-FLAG) antibodies for 1 hour each at room temperature followed by gold conjugated antibodies for 20 minutes. After PBS washes, grids were post fixed with 1% glutaraldehyde for 5 minutes, rinsed with MilliQ water and stained with oxalic acid and uranyl acetate for 5 minutes. After three MilliQ water washes, grids were treated for 2s with methyl cellulose and 5 min with uranyl acetate. Excess stains were removed and samples were imaged using a Talos L120C transmission electron microscope (ThermoFisher Scientific).

Circular dichroism (CD)

CD spectra were recorded for all reactions using a JASCO-1700 CD spectrophotometer with a Peltier temperature controller and in a 0.1 cm path length quartz cuvette. For folding

confirmation, oligonucleotides were prepared at 50 μM in folding buffer (10 mM HEPES, pH 7.5, and 100 mM KCl), heated at 95 °C for 5 minutes, and allowed to cool slowly to room temperature overnight to promote G4 formation. These folded oligos were used to verify G4 structure formation prior to electrophoretic mobility shift assays (EMSAs). For unfolding assays, G4 oligos (either rDNA or cMYC G4 sequences) were folded at room temperature in 20 mM sodium phosphate buffer (pH 7.5) to a final concentration of 5 μM in the reaction mixture. Full-length Gar2 was added at varying concentrations to assess their effect on G4 unfolding. In one set of experiments, cMYC G4 was incubated with a single concentration of each mutant. CD spectra were recorded from 350 to 210 nm, and each spectrum represents the average of three scans. Corresponding buffer spectra were subtracted from each reading. The CD signal (in millidegrees) was converted to molar circular dichroism, data were smoothed and plotted using GraphPad Prism.

Electrophoretic mobility shift assay (EMSA)

Various G4 and non-G4 DNA/RNA substrates were labeled at their 5´ end with either ^{32}P or Cyanine 5 (Cy5) fluorophore (Supporting Table S2). Radioactively labeled substrates were used at a final concentration of 1 nM, while Cy5-labeled substrates were used at a final concentration of 5 nM. Wild-type Gar2 protein and its truncated variants were titrated at increasing concentrations (10-360 nM) in a reaction volume of 20 μl to examine their binding affinities toward different G4 structures, with comparisons made to the corresponding single-stranded substrates. Binding reactions were incubated at 30 °C for 15 minutes. Samples were then subjected to electrophoresis in 10 % native polyacrylamide gels (supplemented with 30 mM KCl) for one hour at 100 V at 4 °C. The running buffer consisted of 0.5X TBE (pH 8.0) supplemented with 50 mM KCl to maintain G4 structure stability. Following electrophoresis, resolved bands were detected using Cy5 fluorescence settings and imaged with Typhoon FLA 7000 phosphorimager (GE healthcare). For ^{32}P labeled oligos, the gel

was dried onto Whatman paper, exposed overnight to a phosphorimaging screen (Fujifilm), and subsequently visualized using a Typhoon 9400 Variable Mode Imager (GE Healthcare).

Microscale thermophoresis (MST)

Binding affinities between various G4 structures and wild type Gar2 were determined by MST using Monolith NT.115 instrument (NanoTemper Technologies). Reactions were performed according to the manufacturer's instructions. Briefly, unlabelled ligand was serial diluted in MST buffer (50 mM Hepes, pH 7.6, 30 mM KCl, 0.25 mg/ml BSA, 0.05% Tween20). Each dilution was mixed with an equal volume of 80 nM Cy5-labeled target (either a G4 or a single-stranded non-G4 control oligonucleotide), resulting in a final volume of 20 µl. The reactions were incubated at 30 °C for 15 minutes and centrifuged at 10,000 rpm for 5 minutes. The samples were aspirated into Monolith standard capillaries. Put the capillaries onto sample tray and scanned them at 25 °C using Nano-Red filter, medium MST power and 30 % excitation. The raw data from instrument was exported and binding curves were generated and fitted using a dose-response model based on the Hill equation in GraphPad Prism.

G4 unwinding trap assay

The Cy5-labeled G4 oligonucleotide substrate was prepared at a final concentration of 5 nM in a buffer (50 mM Hepes pH 7.5, 50 mM KCl, 2mM $MgCl_2$, 0.25mg/ml BSA). The unwinding reaction was started by adding 10 nM of Gar2 protein and 2.5 nM of Trap oligonucleotide (Supplementary Table S2). The reaction was incubated at 30 °C for 20 minutes. At regular time intervals 10 µl of the reaction was taken out and quenched immediately by adding to 10 µl of stop solution (40 % glycerol, 60 mM EDTA, 0.6% SDS, 0.1 µM anti-trap oligonucleotide). The samples were resolved at 120 V for 120 minutes in a 20 % polyacrylamide gel containing 10 mM KCl. Resolved bands were detected using Cy5

fluorescence settings and imaged with Typhoon FLA 7000 phosphorimager (GE Healthcare). The band intensities were quantified by ImageQuant software.

Structure superposition

Alphafold models for *S. pombe* Gar2 (UniProt P41891) and human NCL (UniProt P19338) were downloaded as pdb files from the Aphafold Protein Structure Database. Structures were aligned using ChimeraX 1.11.1 MatchMaker (Needleman-Wunsch, BLOSUM-62), yielding alignment score 785 and core RMSD 0.172 Å (57 pairs) versus an overall 55.238 Å (479 pairs). Per-residue Cα RMSD (seq-rmsd attribute) was visualized via Render by Attribute (Blue 0-1 Å, white 1-3 Å, red >3 Å; missing residues lime green). Individual panels in Fig. S7 show the Gar2 structure (Fig S. 7A), full superposition of Gar2 (sky blue) and NCL (yellow) (Fig. S7B), and superposition in RMSD colour (Fig. S7C). For clarity, Gar2 is hidden and only NCL is shown in RMSD color (Fig. S7C).

Supplementary Tables

Table S1. List of *E. coli* and yeast strains used in this study.

Species	Name	Genotype	Reference
E. coli	DH5 α	F– φ80lacZΔM15 Δ(lacZYA-argF)U169 recA1 endA1 hsdR17(rK– mK+) phoA supE44 thi-1 gyrA96 relA1 λ–	Protein expertise platform, Umeå University
E. coli	Gar2/pET24d/Rosetta (DE3)	F^- ompT $hsdS^B(r^{B-}\ m^{B-})$ gal dcm λ(DE3) [pRARE (Cam^R)] [pET24d-Gar2 (Kan^R)]	This study
E. coli	Gar2 F>A/pET24d/Rosetta (DE3)	F^- ompT $hsdS^B(r^{B-}\ m^{B-})$ gal dcm λ(DE3) [pRARE (Cam^R)] [pET24d-Gar2F>A (Kan^R)]	This study
E. coli	Gar2 R>A/pET24d/Rosetta (DE3)	F^- ompT $hsdS^B(r^{B-}\ m^{B-})$ gal dcm λ(DE3) [pRARE (Cam^R)] [pET24d-Gar2R>A (Kan^R)]	This study
E. coli	R1R2RGG/pET24d/Rosetta (DE3)	F^- ompT $hsdS^B(r^{B-}\ m^{B-})$ gal dcm λ(DE3) [pRARE (Cam^R)] [pET24d-Gar2R1R2RGG (Kan^R)]	This study
E. coli	R1R2/pET24d/Rosetta (DE3)	F^- ompT $hsdS^B(r^{B-}\ m^{B-})$ gal dcm λ(DE3) [pRARE (Cam^R)] [pET24d-Gar2R1R2 (Kan^R)]	This study
S. pombe	Wild type *S. pombe*	972 h-	JCF1, J. Cooper lab
S. pombe	Gar2-HA strain	h- gar2-3xHA::kanMX6	This study

Table S2. List of oligonucleotides used in this study.

Name	Sequence 5'-3'	Source
Cy5_A10-rDNA-G4	Cy5-AAAAAAAAAAGGGGAAGGGTGGGGCATGTTATGGG	*S. pombe*
Cy5_A10-rDNA-M4	Cy5-AAAAAAAAAAGTGGAAGTGTGGTGCATGTTATGTG	*S. pombe*
A10-rDNA-G4	AAAAAAAAAAGGGGAAGGGTGGGGCATGTTATGGG	*S. pombe*
Cy5_NRAS rG4	Cy5-UGUGGGAGGGGCGGGUCUGGGUGC	Human
Cy5_NRAS M4	Cy5-UGUAGAAAGAGCAGAUCUAGAUGC	Human
Cy5_Pu24T_c-MYC	Cy5-TGAGGGTGGTGAGGGTGGGGAAGG	Human
Cy5_(G4C2)4	Cy5-GGGGCCGGGGCCGGGGCCGGGGCC	Human
Cy5_24TTG_htel	Cy5-TTGGGTTAGGGTTAGGGTTAGGGA	Human
c-MYC	TGAGGGTGGGGAGGGTGGGGAA	Human
rDNA-G4_Trap	CCCATAACATGCCCCACCCTTCCCC	*S. pombe*
rDNA-G4 anti Trap	GTGGAAGTGTGGTGCATGTTATGTG	*S. pombe*

Supplementary Figures

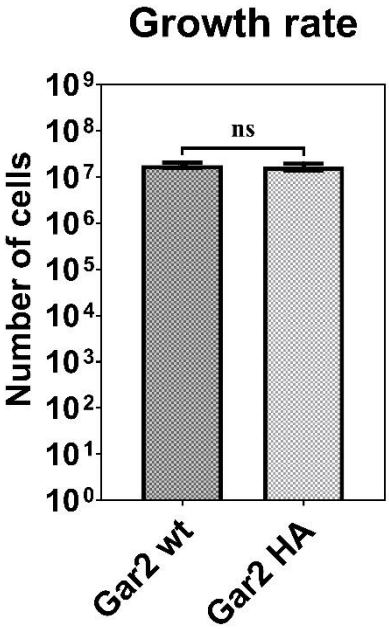

Fig. S1. Effect of 3xHA epitope-tag at the C-terminus of endogenous Gar2. Comparison of growth rate of wild type and Gar2-HA strains of *S. pombe* in YES medium. Growth was measured across three independent experiments, and the data were analyzed by using unpaired t-test ($p = 0.05546$).

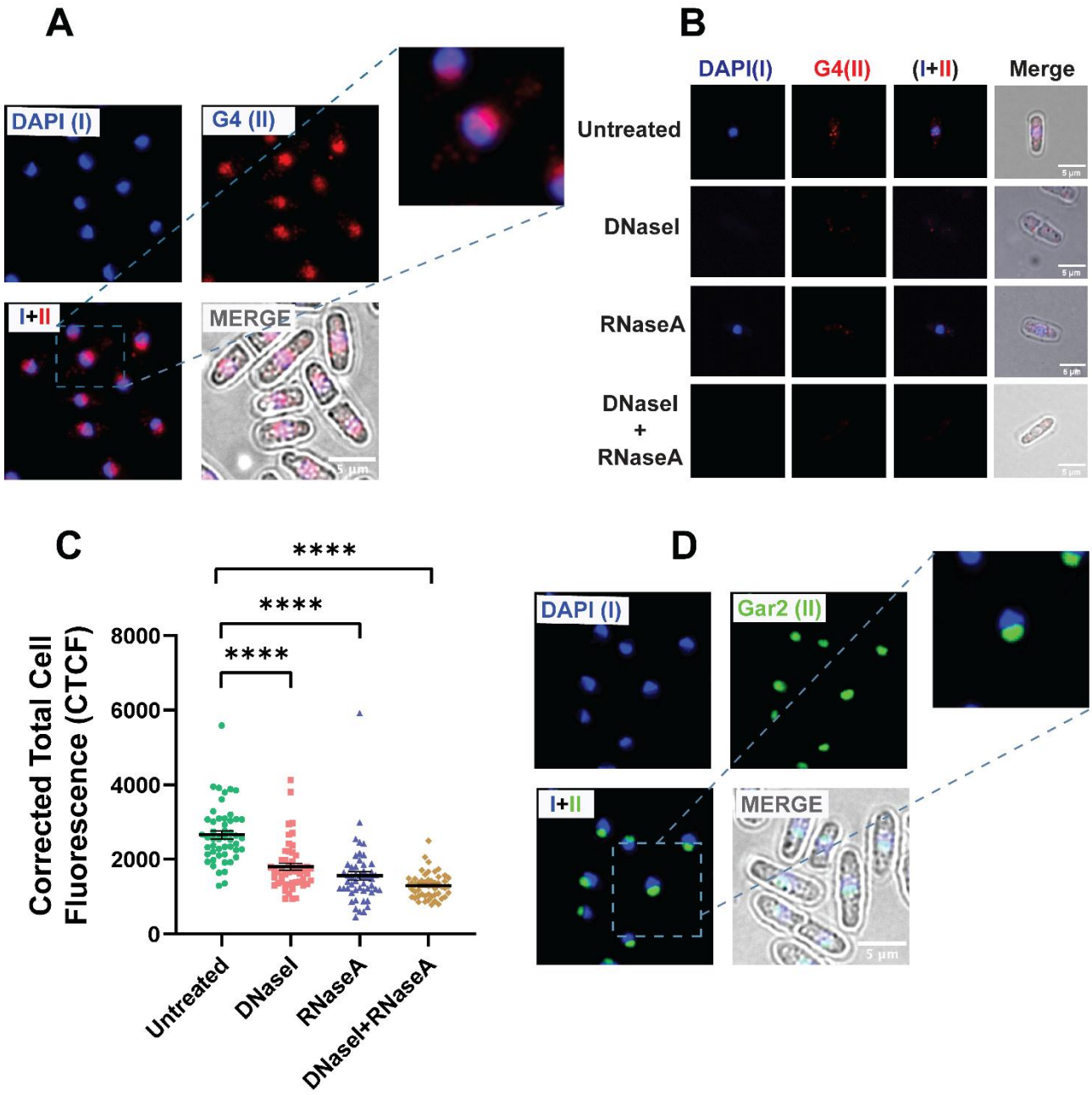

Fig. S2 Localization of Gar2 and G4 in fixed *S. pombe* cells by immunofluorescence microscopy. (A) BG4 antibody staining reveals localization of G4s in both the nucleus and the cytoplasm. The inset shows magnified view of a selected cell. (B) The specificity of BG4 staining in *S. pombe* with nuclease treatment was assessed. Cells were either untreated or treated with DNase I, RNase A, or both DNase I and RNaseA prior to immunofluorescence staining. (C) The corrected total cell fluorescence intensity of BG4 staining was quantified from 25 randomly selected cells per treatment group in each of two independent biological replicates using ImageJ. Data are presented as scatter dot plots with mean ±SEM. Statistical analysis was performed using two-way ANOVA. ****$p < 0.0001$ compared to untreated control. (D) Immunostaining of the Gar2-HA strain with anti HA antibodies shows prominent nuclear localization of Gar2. The inset shows Gar2 localization in a selected cell.

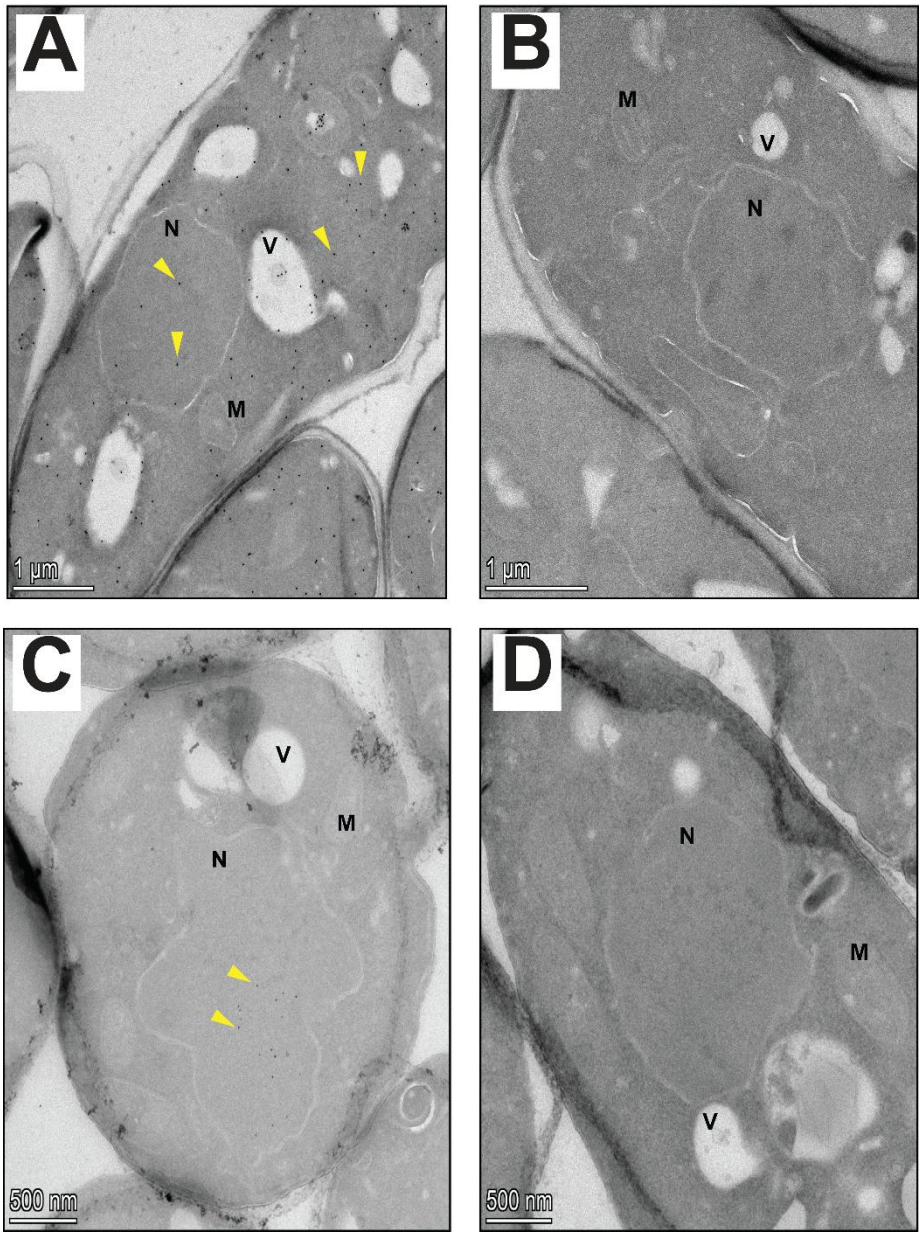

Fig. S3 Localization of either G4 or Gar2 by immunoelectron microscopy.
(A, B) Immunoelectron micrographs of *S. pombe* cells showing G4 localization. (A) Wild type cells incubated with BG4 primary antibodies followed by 15 nm gold-conjugated secondary antibodies display G4 signals in both the nucleus and cytoplasm. (B) Wild type cells incubated with 15 nm gold-conjugated secondary antibodies alone show no detectable signal, indicating specificity of gold-conjugated antibodies. (C, D) Immunoelectron micrographs showing Gar2 localization. (C) Gar2-HA expressing cells incubated with anti-HA antibodies followed by 10 nm gold-conjugated exhibit specific signal in the nucleus, consistent with known Gar2 localization. (D) Wild type cells lacking the HA-tag show no detectable signal, confirming specificity for the HA epitope-tag. Abbreviations: N = nucleus, M = mitochondria, V = vacuole).

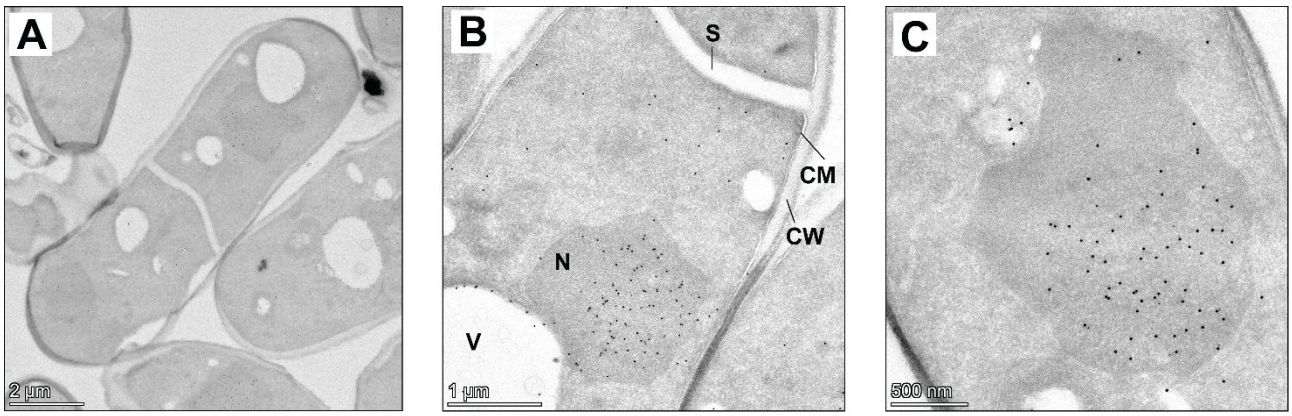

Fig. S4 Colocalization of Gar2 with G4 structures. Micrographs showing colocalization of Gar2 with G4s at different magnifications. G4s were detected using secondary antibodies conjugated to 15 nm gold particles (larger dots), while Gar2 was detected with secondary antibodies conjugated to 10 nm gold particles (smaller dots). G4s were observed in both nucleus and cytoplasm, whereas Gar2 localization was primarily nuclear. Scale bar: 2 µm (A), 1 µm (B), 500 nm (C). Abbreviations: N=nucleus, M=mitochondria, V=vacuole, CM=cell membrane, CW=cell wall, S=septum

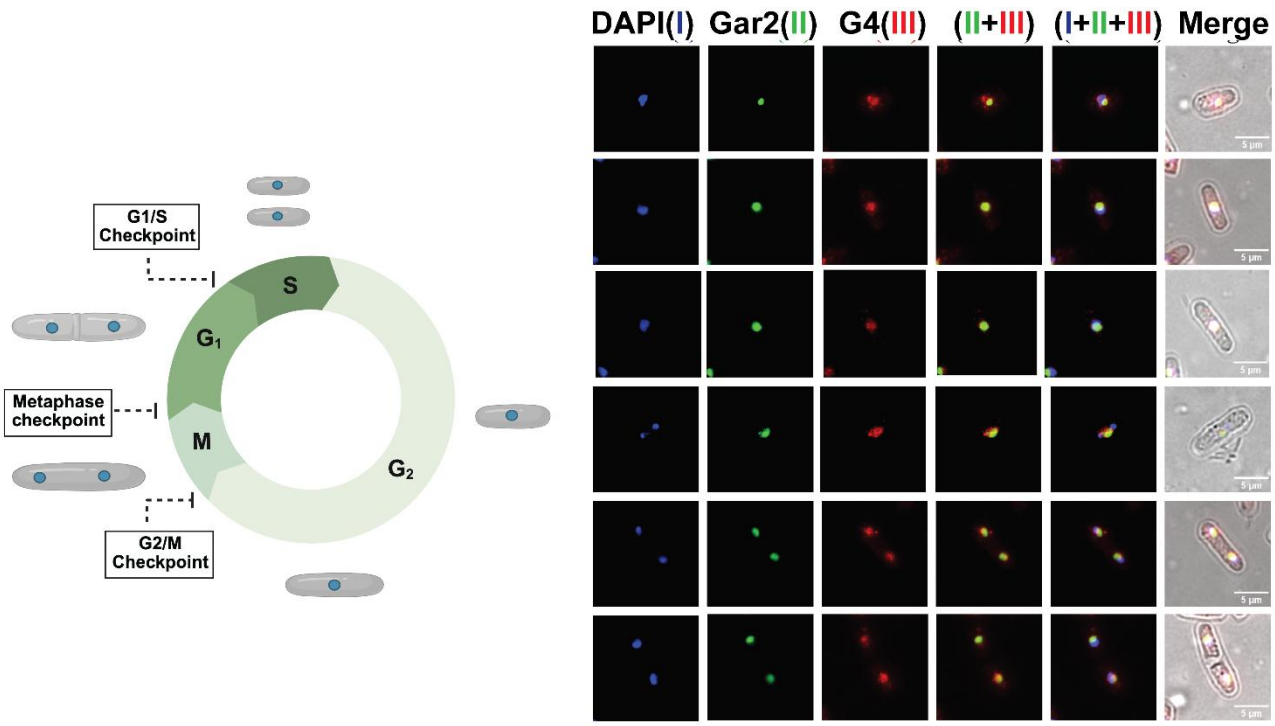

Fig. S5. Colocalization of Gar2 with G4s in *S. pombe* cells of varying lengths. (A) Schematic representation of the *S. pombe* cell cycle. Created in BioRender. Sabouri, N. (2026) https://BioRender.com/co8bl5l (B) Representative immunofluorescence images of cells with varying lengths (a proxy for cell cycle stages). Selection was based on cell length and number of nuclei/genetic material from a single, non-synchronized culture. Colocalization of Gar2 with G4s is observed throughout the population, with varying colocalization intensity patterns.

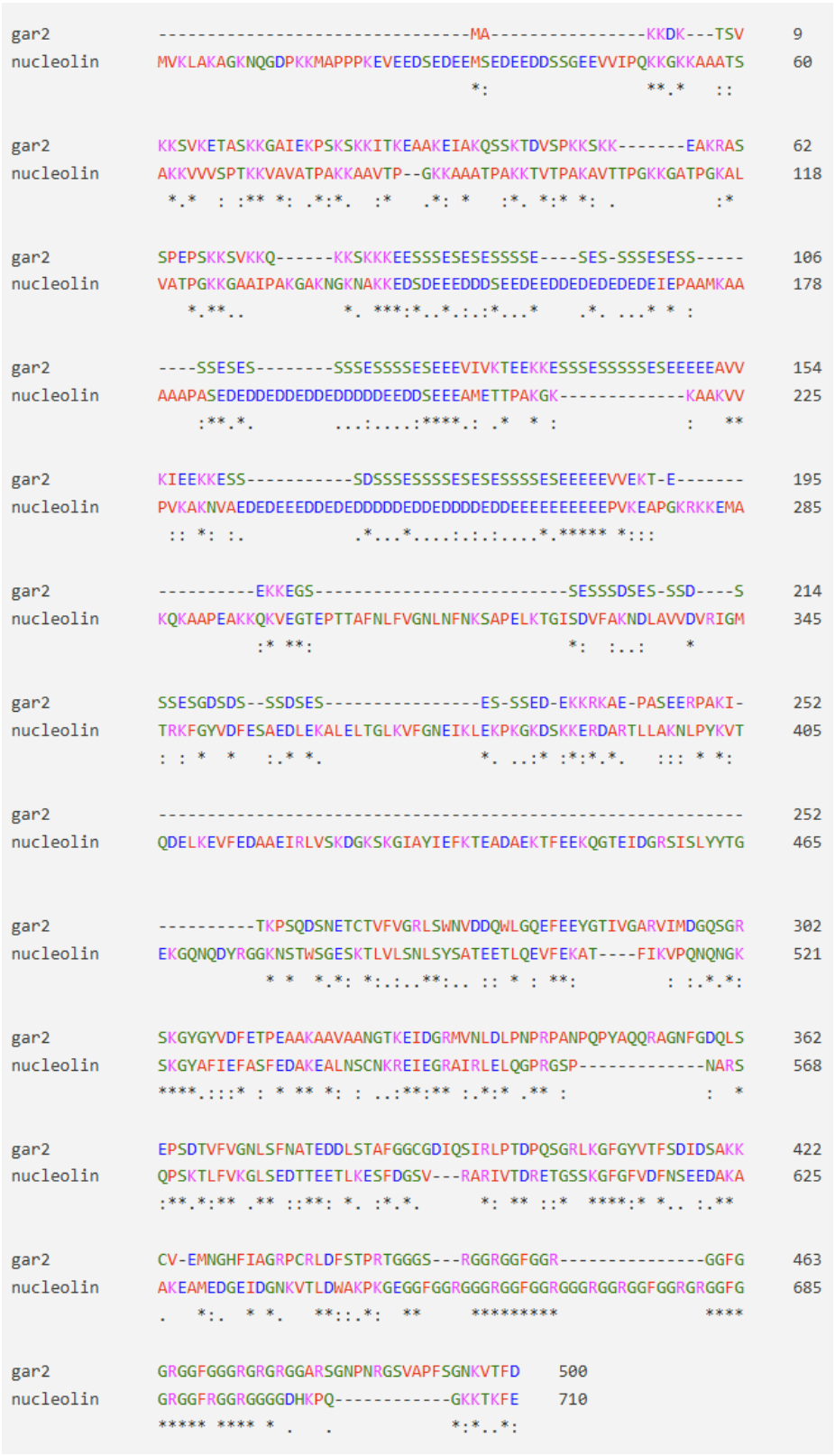

Fig. S6 Sequence alignment of Gar2 with Human Nucleolin using Clustal Omega. Multiple sequence alignment of Gar2 and Nucleolin generated using Clustal Omega. Conserved residues are highlighted, with identical residues indicated by asterisks (*), conserved substitutions by colons (:), and semi-conserved substitutions by periods (.).

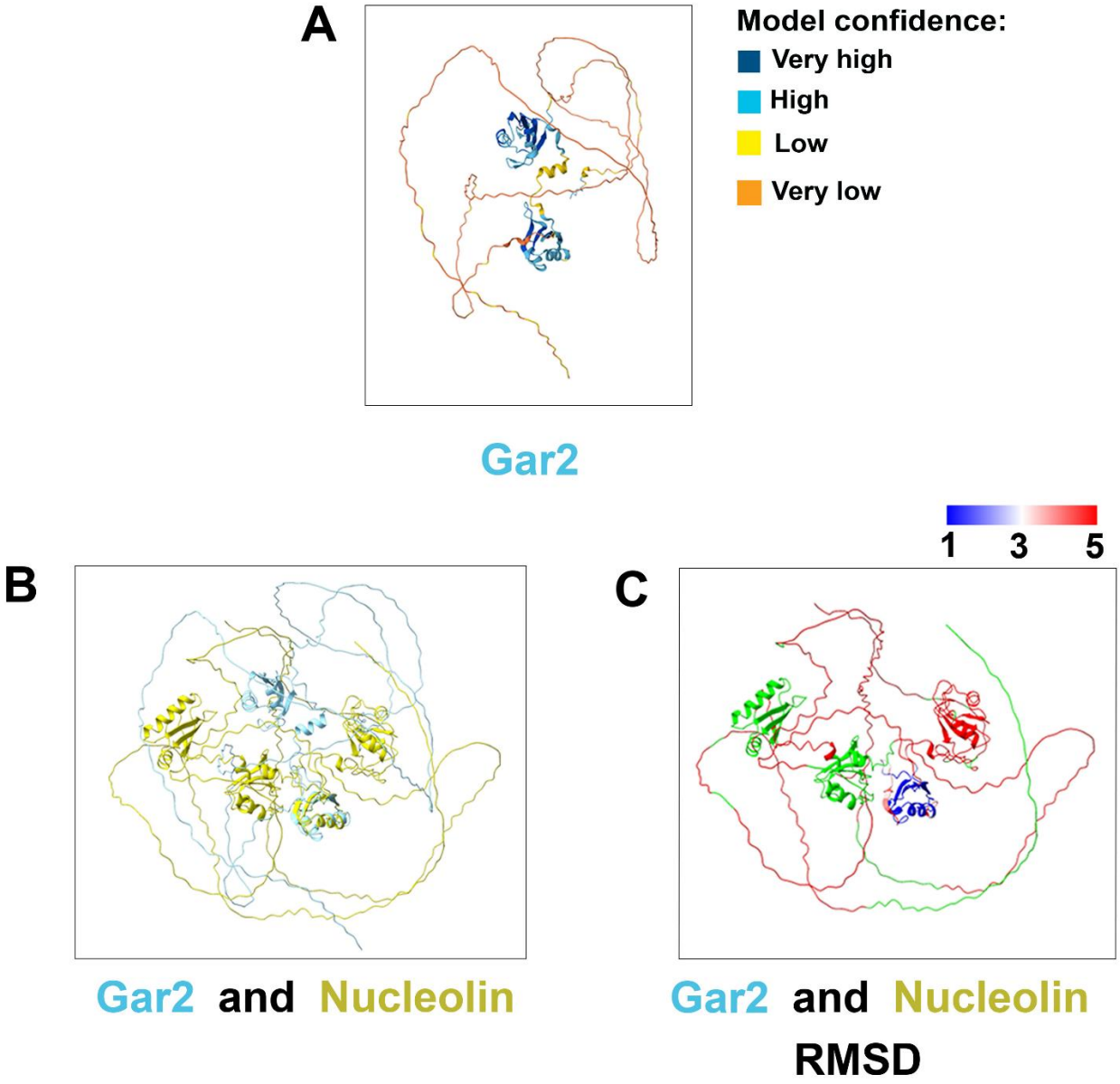

Fig. S7 Alphafold structure comparisons. (A) Alphafold structure of Gar2. (B) Superposed models of Gar2 (sky blue) and nucleolin (yellow) highlight flexible regions flanking conserved cores. (C) Nucleolin is colored by per-residue RMSD relative to Gar2; missing residues are shown in lime green. RMSD scale is displayed above.

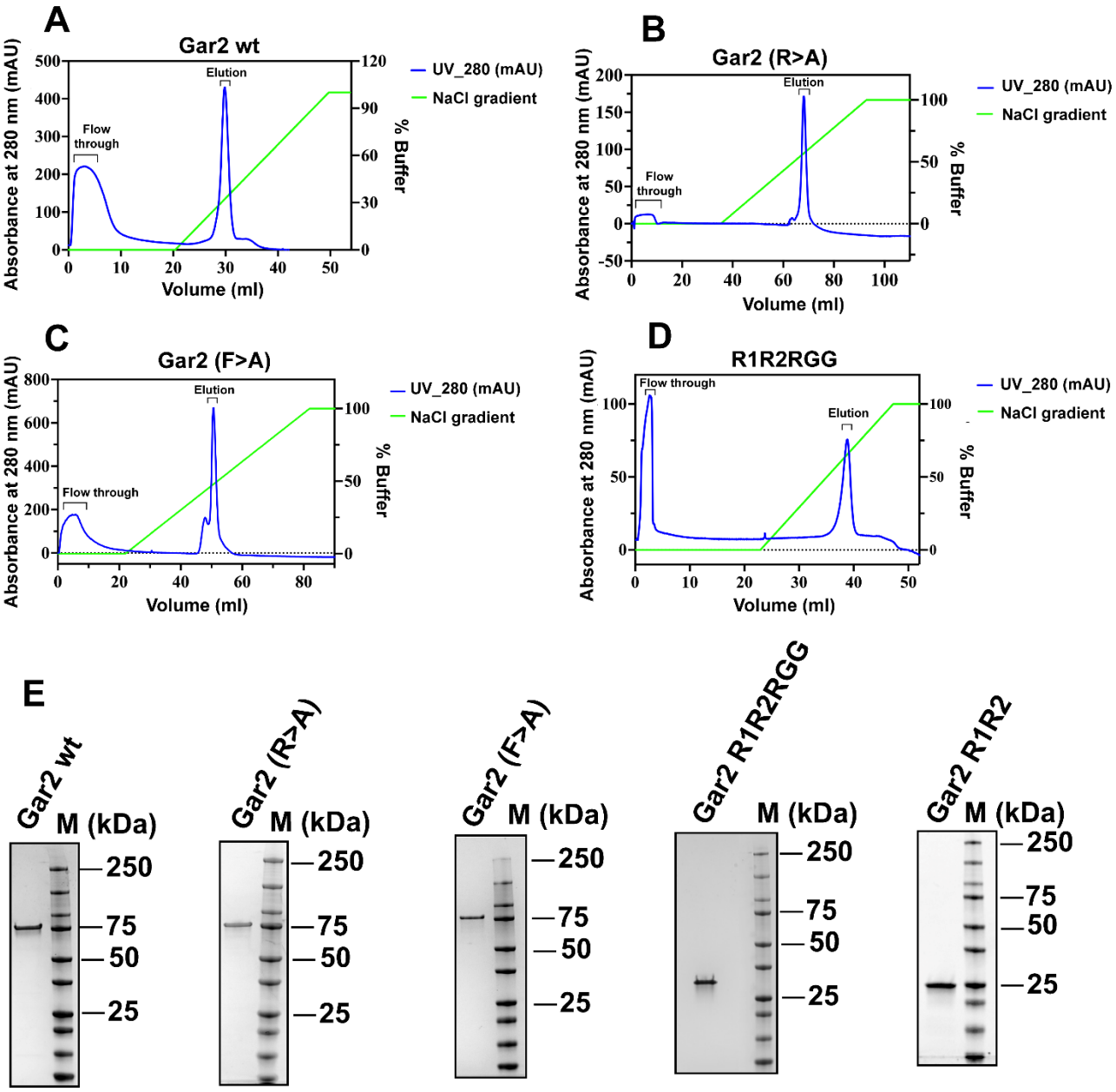

Fig. S8 Purification profiles of various recombinant proteins used in *in vitro* studies. (A–D) His_6-tagged proteins were purified using Ni-NTA affinity chromatography followed by heparin affinity chromatography. All proteins bind to heparin beads except for the R1R2 deletion mutants. Elution was performed using a gradient of NaCl. The chromatograms show the elution profiles from the heparin affinity purification. (E) SDS-PAGE analysis of the purified proteins stained with Coomassie Brilliant Blue, showing bands corresponding to the respective proteins.

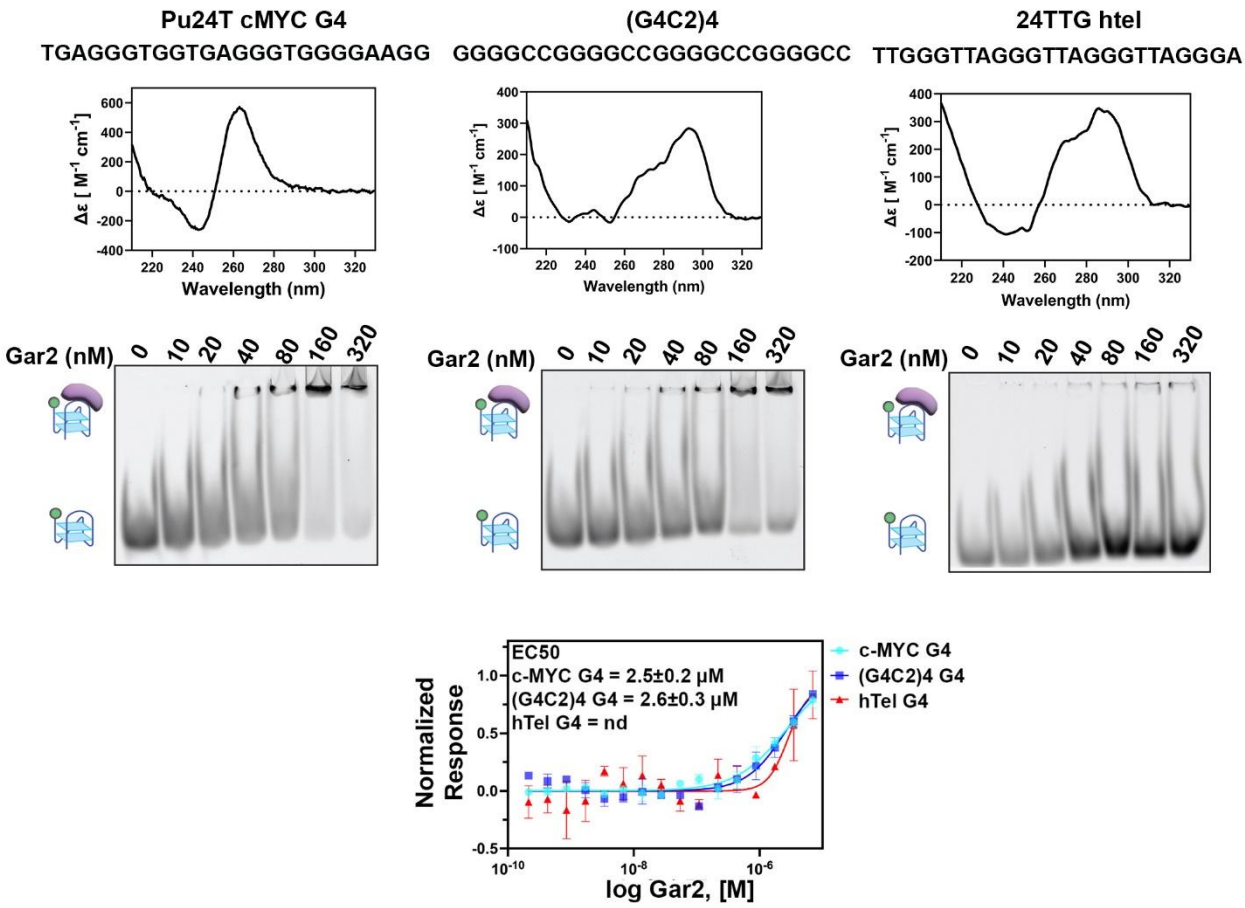

Fig. S9 (A) Circular dichroism spectra depicting the topologies of various G4s used in EMSA. (B) EMSA assay showing the binding of Gar2 to various G4 sequences. (C) Quantification of Gar2 binding affinity toward different G4 sequences using MST. Each MST experiment includes two independent replicates and EC50 is calculated by Hill equation.

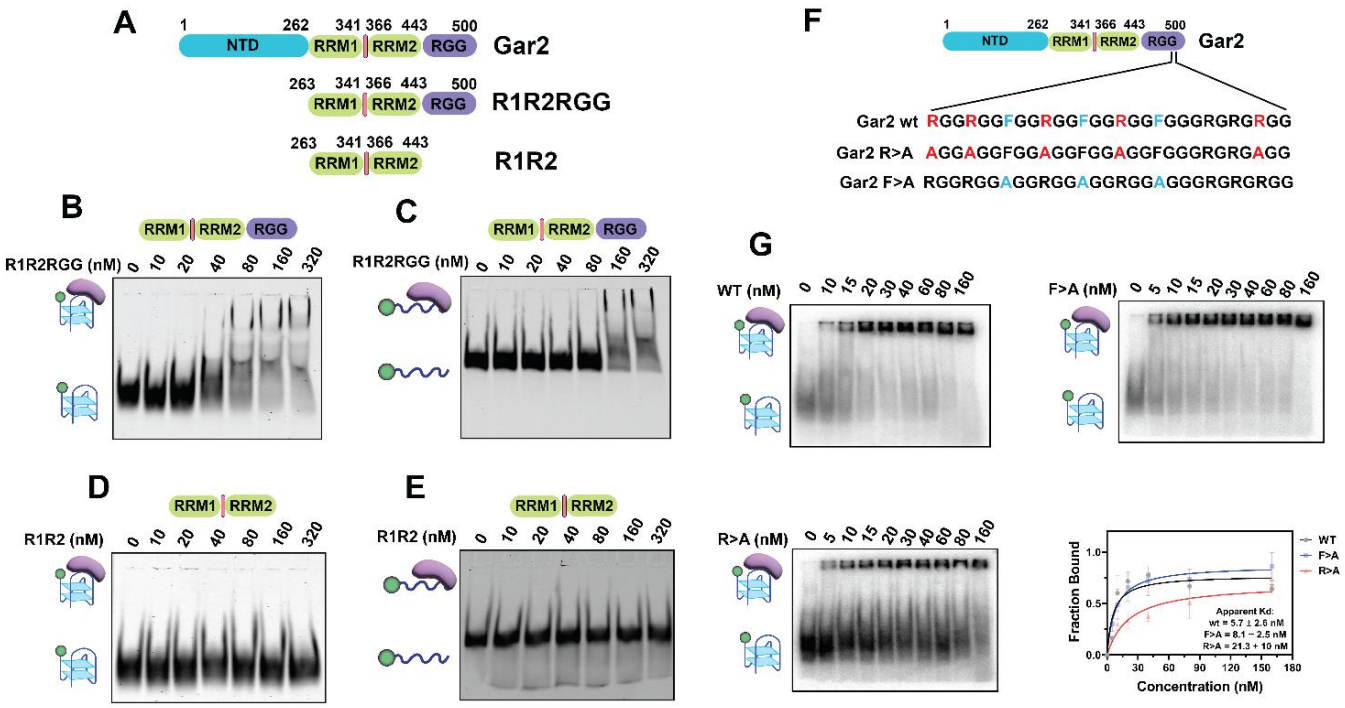

Fig. S10 (A) Schematic diagram illustrating the domain organization of Gar2 and its deletion mutants R1R2RGG and R1R2. (B, C) EMSA showing the binding affinity of R1R2RGG with rDNA G4 and rDNA M4 respectively. (D, E) EMSA showing the binding affinity of R1R2 to rDNA G4 and rDNA M4 respectively. (F) Schematic diagram depicting the positions of arginine (R) and phenylalanine (F) residues in the RGG domain of Gar2 that were substituted with alanine. (G) EMSA comparing the binding of Gar2 (wt) and its mutants R>A and F>A to ^{32}P-labeled rDNA G4. Data were collected from two replicates and fitted to a one-site specific binding model using nonlinear regression in GraphPad Prism.

References

1. G. Biffi, D. Tannahill, J. McCafferty and S. Balasubramanian, Nat Chem, 2013, 5, 182-186.
2. J. Lyu, R. Shao, P. Y. Kwong Yung and S. J. Elsasser, Nucleic Acids Res, 2022, 50, e13.
3. J. Bahler, J. Q. Wu, M. S. Longtine, N. G. Shah, A. McKenzie, 3rd, A. B. Steever, A. Wach, P. Philippsen and J. R. Pringle, Yeast, 1998, 14, 943-951.
4. S. K. Rai, A. Atwood-Moore and H. L. Levin, Methods Mol Biol, 2018, 1721, 167-177.
5. I. M. Hagan, Cold Spring Harb Protoc, 2016, 2016.
6. K. K. Yan, I. Obi and N. Sabouri, Nucleic Acids Res, 2021, 49, 8339-8354.
7. B. Herdy, C. Mayer, D. Varshney, G. Marsico, P. Murat, C. Taylor, C. D'Santos, D. Tannahill and S. Balasubramanian, Nucleic Acids Res, 2018, 46, 11592-11604.
8. A. Tawani, S. K. Mishra and A. Kumar, Sci Rep, 2017, 7, 3600.
9. Y. Zhang, J. Huang, K. Yu and X. Cui, Molecules, 2023, 28.
10. S. Bielskute, J. Plavec and P. Podbevsek, J Am Chem Soc, 2019, 141, 2594-2603.
11. T. Masuzawa and T. Oyoshi, ACS Omega, 2020, 5, 5202-5208.